

# An Integrated Study of Reservoir-Induced Seismicity and Landsat Imagery at Lake Kariba, Africa

A combined study of reservoir-induced earthquakes and Landsat Imagery yields information on geology and tectonics that either alone would not provide.

## INTRODUCTION

**E**ARTHQUAKES, depending upon their depth of origin and geographic location, are the result of different types of physical mechanisms. Perhaps the most interesting occurrences of earthquakes are those linked, both directly and indirectly, to the actions of men. Examples

threat to life and property; (2) they offer a unique class of earthquakes which may be prevented, controlled, and possibly predicted; (3) they provide a class of earthquakes that can be easily monitored; and (4) the understanding of the physics of these earthquakes would offer clues regarding the nature of other classes of shallow earthquakes.

---

**ABSTRACT:** *The depth and seismic source parameters of the three largest reservoir-induced earthquakes associated with the impoundment of Lake Kariba, Africa, were determined using a formalism of the generalized inverse technique. The events, which exceeded magnitudes,  $m_b$ , of 5.5, consisted of the foreshock and main event (0640 and 0901 GMT, 23 September 1963) and the principal aftershock (0703 GMT, 25 September 1963). Landsat imagery of the reservoir region was exploited as an independent source of information to determine the active fault location in conjunction with the teleseismic source parameters. The epicentral proximity and the comparable source parameters of the three events suggests a common normal fault with an approximate strike of S 9°W, a dip of 62°, and rake of 266°. The fault transects the reservoir's deep Sanyati Basin. Body-wave modeling of the events infers source depths of less than 10 km. The photointerpretation of Landsat imagery resulted in the mapping of over 400 lineaments, having trends of N 20°W to N 40°W, that transect the Mid-Zambezi Rift Valley region. These features seem to be correlated with joint fracture patterns and dykes injected with Precambrian pegmatites and Jurassic dolerites. The lineaments and their intersections with known faults may provide potential sites for future mineral exploration.*

---

would include earthquakes triggered by subsurface nuclear explosions, subsurface injection of fluids, and the construction of man-made reservoirs (Gupta and Rastogi, 1976; Healy *et al.*, 1972; Dahlman and Israelson, 1977; Gough, 1978). Earthquakes generated by cultural activities are of particular interest to the seismological community because (1) they may pose a serious

This study is concerned with the nature of reservoir-induced seismicity (RIS) presumably caused by the impoundment of Lake Kariba in southern Africa. The geographical location of Lake Kariba and the generally small to moderate size of the earthquakes which occurred there are factors which have limited previous seismological investigations. In the present study, we have

endeavored to use recently developed seismological techniques in conjunction with interpretation of Landsat imagery to determine basic fault parameters such as source depth, fault orientation, and epicenter location. The rationale behind this is eventually to build a catalog of accurately determined source parameters from reservoir-induced earthquakes to be used in assessing possible physical mechanisms relevant to the phenomenon of induced seismicity.

#### THE PROBLEM OF RESERVOIR-INDUCED SEISMICITY (RIS)

Reservoirs have been constructed throughout the world for many reasons including hydroelectric power, flood control, irrigation, commerce, and recreation. Site selection of these reservoirs is principally a function of the structural, geological, and hydrological properties of the region within which the reservoir is to be impounded. A small proportion of the hundreds of reservoirs constructed during the past century have been associated with a change in regional earthquake activity. In a few documented instances, RIS has achieved catastrophic proportions, which resulted in damage to the dam structure, extensive property damage, and loss of human life. An extreme example is the Koyna Reservoir of India, which is believed to have triggered the magnitude 6.4 earthquake which occurred there in 1967. Simpson (1976) and Gupta and Rastogi (1976) provide excellent reviews of the RIS phenomenon that was first observed at Lake Mead, Arizona, in the 1930's, by Carder (1945).

Reservoirs associated with the RIS phenomena have some common features. RIS is most commonly associated with large reservoirs; large reservoirs being defined as having a volume in excess of a million-acre feet ( $1.2 \times 10^9 \text{ m}^3$ ) and impounded behind a dam in excess of 90 metres (Simpson, 1976). Perhaps the key feature of RIS is that, typically, the earthquake frequency of the region increases measurably following the filling of the lake. Epicenters are usually located within 25 km of the reservoir. By correlating the frequency of the earthquakes' occurrence with the fluctuations in reservoir water level, Gupta *et al.* (1972) suggested that the following factors affected the frequency of seismicity: the rate of increase in water level; duration of loading; maximum levels of water; and the time period for which the high water levels were maintained. Finally, some investigators have inferred that certain geological and hydrological conditions are necessary for such earthquake occurrences. Case histories of the Koyna (India), Kariba (Zambia-Zimbabwe), and Kremasta (Greece) reservoirs provide evidence that pore pressure changes, permeability, porosity, and pre-impoundment water table levels play important

roles in the actual physical mechanisms of RIS (Gupta and Rastogi, 1976; Brace, 1972; Healy *et al.*, 1972; Wahlstrom, 1974).

Some investigators have addressed the nature of the actual triggering mechanisms acting at depth within the Earth's crust beneath the reservoir. Gough and Gough (1970b) initially identified three mechanisms by which seismic activity could be potentially stimulated by the loading of an artificial lake; (1) the direct effect of the increase in shear stress at depth; (2) the indirect effect of incremental stress in 'triggering' release of pre-existing tectonic stress; and (3) the effect of increased pore pressure acting upon dormant fault zones beneath the reservoir. Through their study of the stresses induced by the impoundment of Lake Kariba, Africa, Gough and Gough (1970a, 1970b) dismiss the mechanism attributed to the direct load-induced increase in shear stress. Furthermore, RIS depends upon the type of faults that may exist beneath the reservoir; i.e., dip-slip normal, strike slip, or thrust faults. Kisslinger (1976) provides a comprehensive review of the mechanisms for reservoir-induced earthquake activity. More detailed analysis of the role of pore pressure as a possible triggering mechanism has been reported by Bell and Nur (1978).

Within the scope of determining the mechanism of reservoir-induced earthquakes, seismological techniques have been utilized to constrain the parameters that define the orientation and depth of the fault plane upon which the reservoir-induced earthquakes occur. The fault plane orientation is conventionally defined by geographic location, depth, and the angular parameters of strike,  $\theta$ , dip  $\delta$ , and rake,  $\lambda$ . By constraining the fault or dislocation parameters, including the depth of the given earthquake(s), complemented by ancillary information of the hydrological, geological, and tectonic environment of the region, it may be possible to deduce the triggering mechanisms acting at depth beneath the reservoir. Achieving an understanding of the triggering mechanism would offer hope for the eventual prevention, control, and possible prediction of the RIS phenomena.

#### LAKE KARIBA, AFRICA

Lake Kariba, which borders Zambia and Zimbabwe-Rhodesia (16.8°S, 28.0°E), is the result of a joint governmental action to develop a source of hydroelectric power for the region. The reservoir occupies the Mid-Zambezi Basin which is considered to be a dormant southern extension of the East African Rift System. The reservoir is formed by the impounded waters of the Zambezi River, as well as other rivers of the watershed region. The impoundment of the Kariba Reservoir began in December 1958 through the operation



FIG. 1. Landsat imagery of the Lake Kariba region. Zambia borders the northern and western shores of the lake. Zimbabwe borders the lake to the south and east. Two images were concatenated to insure total coverage of the reservoir; both images are Band 6, collected on 30 September 1972.

of a dam that was constructed at the mouth of the Kariba Gorge, which is located about 420 km downstream from Victoria Falls. Lake Kariba remains the world's largest artificial lake, extending over 250 km in length and about 30 km in width. Having an area of approximately 6650 km<sup>2</sup>, the lake stores  $1.53 \times 10^{11}$  m<sup>3</sup> of water when the water reaches an engineered maximum level of 484.6 m (1590 ft) above sea level (Gough and Gough, 1970a; McConnell, 1978). Figure 1 is a composite Landsat image, Band 6, of the reservoir. The lake is relatively shallow with an average depth of 18 metres. However, depths exceeding 80 metres are achieved in some areas of the reservoir. Lake Kariba dam is located on the northeastern shore of the lake. The Zambezi River is seen to exit the dam through the Kariba Gorge where it continues northeast through the rift valley. The image, which was employed in the interpretation of geological structure, serves to highlight the reservoir's size.

Gupta *et al.* (1972) indicates that the Lake Kariba region was considered aseismic prior to the impoundment in early 1959. Figure 2, extracted from the Archer and Allen (1979) catalog of earthquakes for the Kariba region, illustrates that, shortly after impoundment, seismicity increased dramatically. As witnessed at other reservoirs associated with RIS, the figure displays the apparent correlation between the changes in the reservoir's water level and the increase in regional seismicity. Comprehensive studies of the seismicity at Lake Kariba have been reported by Gough and Gough (1970a, 1970b). Archer and Allen (1979) provided a comprehensive catalogue of the Kariba tremors of magnitudes  $\geq 2.0$

for the period spanning June 1959 through January 1979.

In September 1963, seismicity dramatically increased to new levels by the triggering of six earthquakes having magnitudes exceeding 5.0 on the Richter scale. Table 1 provides a synopsis of the major earthquakes that have been located within the immediate vicinity of the reservoir. The main event, of magnitude 6.0, caused damage to the dam structure and some property damage in nearby settlements; however, there were no reports of any casualties (Gupta and Rastogi, 1976).

The locations of the larger earthquakes occupy two areas of the reservoir; (1) the 1963 sequence, spanning from September to November, was located by Fairhead and Girdler (1969) beneath the Sanyati Basin; and (2) the 1972 sequence, spanning December 1972 to August 1974, was located in the "neck" region of the reservoir—a straight of water linking the deep Sanyati Basin to the shallower western basin. Figure 3 illustrates the general locations of the earthquake sequences observed at Lake Kariba.

#### GEOLOGY AND STRUCTURE OF THE LAKE KARIBA REGION

Figure 4 illustrates a very simplified geological map of the Kariba region. The map was constructed from a compilation of geological maps which was then projected on a base map generated from 1:250,000 prints of Landsat Band 7 imagery of the region. The map covers the geographical area known as the Mid-Zambezi Basin. The East African Rift System, of which the basin is a part, is thought to have developed from large

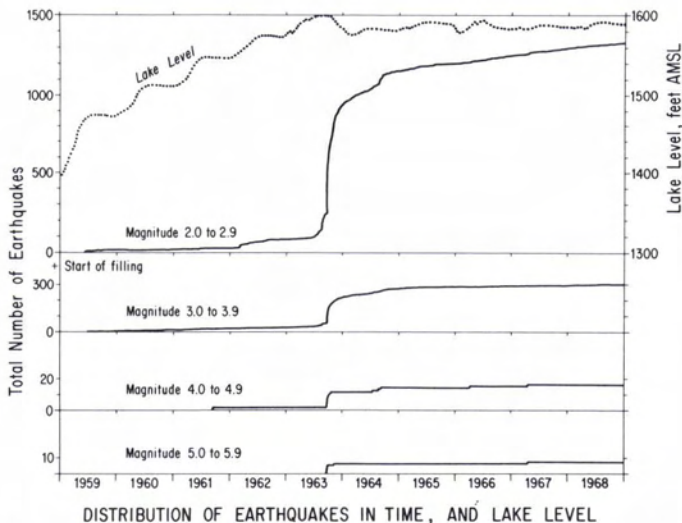


FIG. 2. Correlation of the water level history with the seismic history at Lake Kariba provides standard evidence for the existence of reservoir-induced seismicity. From Archer and Allen (1979).

TABLE 1. SYNOPSIS OF MAJOR EARTHQUAKE ACTIVITY AT LAKE KARIBA

Earthquake Time (GMT)	Magnitude ( $m_b$ )	Location	Depth**
0640 23 Sept 63	5.6	16.69°S 28.43°E	6.0
0810 23 Sept 63	4.9	16.59°S 28.70°E*	8.0
0901 23 Sept 63	6.0	16.58°S 28.46°E*	8.5
1502 23 Sept 63	5.4	16.67°S 28.40°E*	10.0
2223 23 Sept 63	5.3	16.70°S 28.42°E	5.0
0913 24 Sept 63	5.3	16.64°S 28.54°E*	4.0
0703 25 Sept 63	5.8	16.71°S 28.44°E	7.0
0959 8 Nov 63	5.4	16.63°S 28.56°E*	4.5
0251 20 Apr 67	4.9	16.77°S 28.37°E	4.5
0318 12 Dec 72	5.2	16.74°S 28.08°E	5.0
0118 18 Dec 72	5.6	16.71°S 28.07°E	5.0
0605 13 Jan 73	5.3	16.78°S 28.04°E	5.0
0936 1 Aug 74	5.3	16.63°S 27.89°E	5.5

\* Earthquake locations annotated with an asterisk (\*) denote epicentral locations derived by Fairhead and Girdler (1969), through the application of a joint epicentral determination methodology. The remaining epicenters were determined by a relative event location method (Pavlin and Langston, 1982a).  
 \*\* Depths derived from the analysis of surface waves and short period body waves; from Pavlin and Langston (1982b).

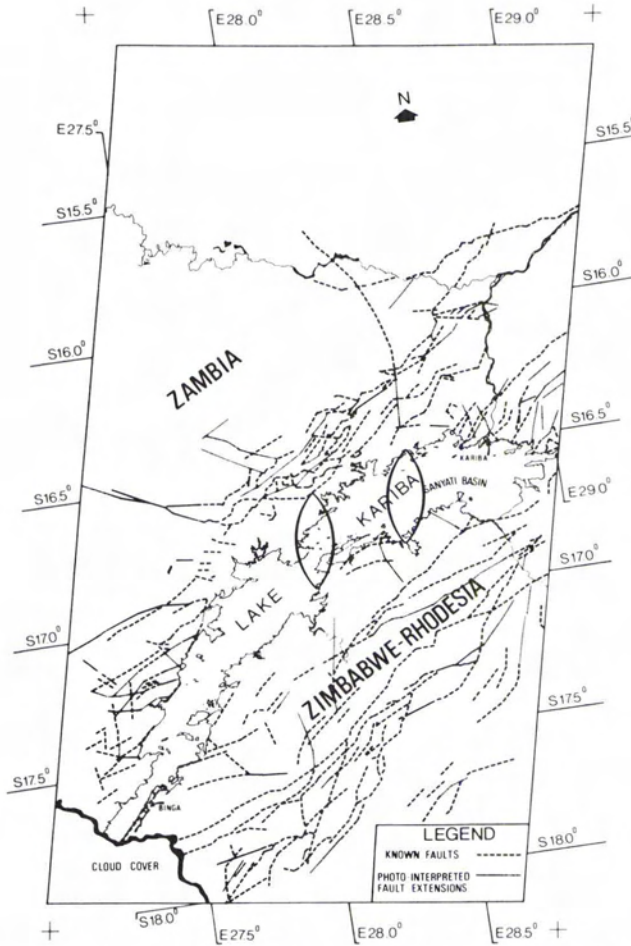


FIG. 3. Compilation of the known faults in the Lake Kariba region. The general zone of significant earthquake activity is annotated with the elliptic graphic patterns. The 1963 sequence is located beneath the Sanyati Basin and the 1972 sequence is located about 50 km to the southeast.

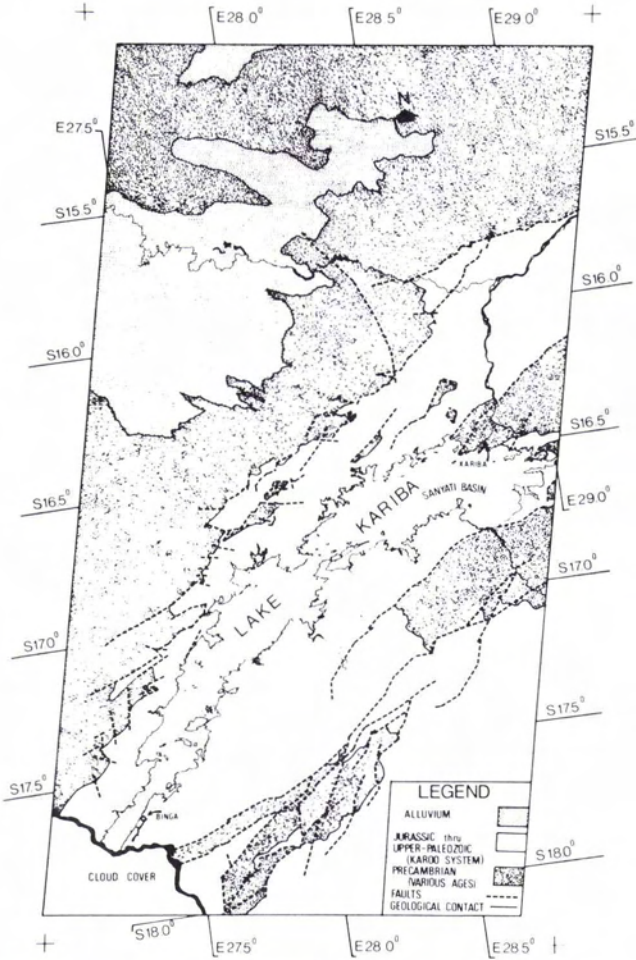


FIG. 4. Geologic Map of the Mid-Zambezi Basin region. Lake Kariba is impounded in a rift valley of the East African Rift System.

scale right-lateral strike-slip faulting during Precambrian time; specifically, the Shamvaian metamorphic event that occurred 2.7 to 2.3 BYR ago (McConnell, 1970). The valley is contained within the Zambezi Metamorphic Belt that extends 900 km along the northern margin of the Rhodesian craton. The craton is relatively undisturbed and radiometrically dated to 3.5 to 2.6 BYR in age (Hurly, 1968).

Since cratonic consolidation, the granites and basalts of the Kariba region have experienced metamorphic diastrophism during four distinct periods: Shamvaian, 2.7 to 2.3 BYR; Magondi, 2.0 BYR; Katangan, 800 MYR; and the Miami, 600 to 400 MYR (pre-Silurian time). These radiometrically dated events have been reported in detail by several investigators, including Hitchon (1958), Stagman (1978), Broderick (1976), and Gair (1959).

Besides the Shamvaian event, the Magondi and Katangan metamorphic events are significant because their ancient tectonic stress fields may control surficial structure observed today (Broderick, 1976). Specifically, the Magondi event produced high grade metamorphism and large scale folding and foliations along northeasterly trends, whereas the Katangan event produced even higher grade metamorphism, folding, and foliation along northwest trends. The structural trends observed in recent times seems to conform to the orientations of the latter structural zones of weaknesses.

The basement rock, which is extensively exposed around the reservoir's perimeter, is typically mapped as Precambrian paragneiss, biotite-quartz gneiss, and schists, all having structural features that trend NE or NW. The basement rock is of variable age; the age is dependent

upon the age of the most recent metamorphic event within the particular region (Snow, 1974; Drysdall and Weller, 1966).

The reservoir is directly in contact with the Upper Paleozoic-Mesozoic units of the Karoo Formation. Within the lake region, these continental sedimentary rocks and lavas are measured to be about 2.8 km thick; however, the units are thought to thin to about 1.9 km immediately beneath the reservoir. Late Permian coal measures constitute the base of the Karoo stratigraphic section. They are overlain by thick accumulations of mudstones and grits. The formation is capped by extensive flood basalts of Jurassic age; however, this unit has been largely eroded in the immediate vicinity of the reservoir. The basalt flows may be linked to the breakup of Gondwanaland (Hurley, 1968; McConnell, 1970; Stagman, 1978). Snow (1974) describes the Karoo's hydrological properties.

Figure 3 illustrates a map of all of the known faults in the Zambia-Zimbabwe border region. The infrared channel, Band 7, of the Landsat imagery of 30 September 1972 provided the base map, due to the channel's optimal discrimination of land and water. Large scale 1:250,000 black-and-white prints of Band 6 imagery were principally utilized to extend the known faults through photointerpretation. As the solar elevation of 53° was not optimal for maximizing contrasts (Holben and Justice, 1980), information provided by the remaining channels was incorporated into the analysis. Imagery collected on 13 August 1976, with a solar elevation of 36°, was also considered in the study. Fortuitously, the solar azimuths of 70° and 55° of the respective images proved optimal for discerning structural features with northwest trends (Sabins, 1978). The latter fact contributed to the discovery of approximately 400 lineaments having trends varying from N 20°W to N 40°W. These lineaments, which may be related to underlying basement structure, were plotted on a separate base map (Figure 5). Rose diagrams for the Kariba region are displayed in Figure 6.

The Mid-Zambezi Basin, as illustrated in Figures 3 and 4, was formed by movement along *en echelon* normal faults trending N 50°E. This fault pattern is believed to have been initiated at the close of the pre-Silurian Miami event (Broderick, 1976). The faults were reactivated in Permian time, coincident with the deposition of the Karoo Formation. The extensive *en echelon* normal faults observed today are largely considered to be an exhumed structural feature (Gair, 1959), although there is considerable evidence to suggest that some faults of the rift valley are still active. Evidence would include the existence of thermal springs (Snow, 1974), recent rejuvenation of streams along the escarpment, and minor earth

tremors in the valley (Gough and Gough, 1970b; Stagman, 1978; Broderick, 1976).

The lineament patterns of the study area, illustrated in Figure 5, have been partially confirmed from geological field studies conducted in areas adjacent to the reservoir; however, there is no ancillary information to confirm the existence of the total pattern. Hitchon (1958) reports that the lineaments observed in the vicinity of the dam do not transect post-Karoo faults. Snow (1974) mentions the existence of northwest trending Precambrian pegmatites and Jurassic dolerites transecting foliated basement rock in the Kariba Gorge region. Additional evidence that the lineaments are real structural features is provided by Smith (1963) and Stagmen (1978).

In comparison to the active region of the East African Rift System to the north, the Mid-Zambezi Basin's evolution as a rift system seems to have diminished since Jurassic time although it still displays some rifting activity (Snow, 1974). Evidence of the region's rift valley nature includes the *en echelon* normal faults (Gair, 1959); the presence of thermal springs and high heat flow in both the local and adjoining areas (Chapman and Pollack, 1977); and the recent seismicity (Archer and Allen, 1979). Undoubtedly, the tectonic environment at Lake Kariba plays a significant role in the triggering mechanism(s) of the earthquakes.

#### SEISMIC ANALYSIS

A striking attribute of the seismic data from Kariba earthquakes is its general poor quality. The sparse distribution of seismic stations in Africa, including the few near Lake Kariba, make the application of standard location and source mechanism techniques equivocal at best. For example, it is well known that the quality of locations derived from ISC (International Seismological Centre) data is only  $\pm 40$  km in the epicenter and in depth (Engdahl and Kanamori, 1980). Clearly, the epicenters of Table 1 have true error bounds on the order of the entire distribution of earthquakes shown in Figures 3 and 5. The *relative* distribution of seismicity is probably better known from the study of Fairhead and Girdler (1969) and our efforts at event relocation, although it is again clear that our interpretation is simply allowed by the data but not required. Problems encountered in deriving useful focal mechanisms from the body-wave *first-motion* data are more severe because a prerequisite for good solutions is a dense distribution of seismic stations in azimuth and distance from an event. Thus, on the face of the poorly distributed data, it first appears that no useful fault parameters can be obtained for the Kariba earthquakes using standard seismological techniques.

A major objective of this study was to overcome many of these problems by using some relatively recent developments in seismic waveform model-

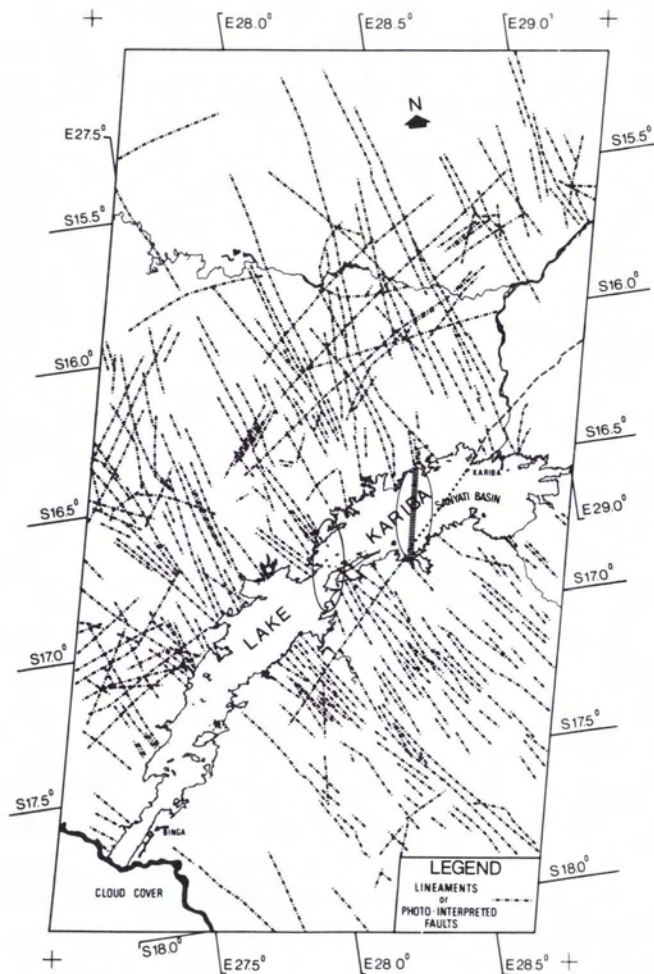


FIG. 5. Compilation of lineaments that were photointerpreted from Landsat imagery of the Lake Kariba region. The lineaments appear to correlate with dykes and joint fracture patterns injected with dolerite and pegmatite during late Precambrian time. Ellipsoid in Sanyati Basin depicts the September 1963 zone of earthquake activity. The dashed line in the ellipse, trending S 9°W, indicates the strike of the active fault as determined from seismic analysis. The dotted line bearing N 50°E, connecting a photointerpreted lineament with a known major fault near Kariba, is the projection of an inferred fault beneath the reservoir.

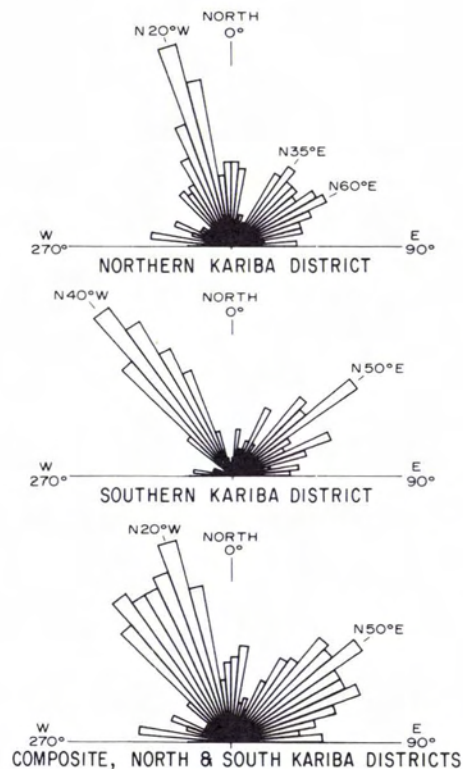


FIG. 6. Rose diagram of lineaments and faults mapped within the Mid-Zambezi Basin region. Nearly all of the known faults have strike azimuths of N 50°E; however, the lineaments' mean azimuth changes by 20° when comparing the northern and southern districts. The two districts are arbitrarily defined to be those areas north and south of Lake Kariba in the Landsat composite.



ing. Those Kariba events of magnitude close to 6.0 were recorded at a number of teleseismic receivers. At teleseismic distances between  $30^\circ$  and  $90^\circ$  from the source, wave propagation in the Earth for P and SH body waves is largely understood. Figure 7 shows a cartoon of Earth structure important in body wave propagation. In this particular distance range rays for body waves bottom in the lower mantle and their response can be easily computed using ray theory. Because the wave propagation is simple, synthetic seismograms for teleseismic stations can be efficiently computed for dislocation sources embedded in layered elastic structure at the source. Theory for these calculations is given by Helmberger (1974), Langston and Helmberger (1975), and Langston (1981).

By using the P and SH waveforms, including their relative amplitudes, a data inversion can be performed to derive the orientation of faulting, seismic moment, source depth, and an estimate of the spatially integrated slip function at the source. Helmberger and Burdick (1979) review many of these studies. It is possible to derive this information from the waveform because it is seen that teleseismic waveforms from shallow earthquakes are the result of the direct and many near-source reflected waves which cause a distinctive interference effect for various source types. Typically, good results are obtained for moderate earthquakes when 10 to 20 P and SH waveforms are simultaneously inverted using a formal generalized inversion procedure (e.g., Wiggins, 1972). In fact, it has also been recently shown (Langston, 1982) that a P and SH waveform from a single station can often significantly constrain the faulting mechanism.

The amount of data for the larger Kariba shocks fell between these two levels. In general, there were enough data to obtain good modeling results but not quite enough to be sure of data consistency. For example, it would always be desirable to have an azimuthally distributed data set so that smooth azimuthal changes in waveshapes could be seen directly. This is not always possible with sparse data sets. Nevertheless, with the application of these techniques it became possible to obtain source parameters which were previously lost in the noise of less robust methods. The analysis of Landsat imagery attained a central role in this work by providing additional support for derived mechanisms and in placing possible constraints on epicentral location.

## RESULTS

Utilizing long and short period body-wave data of the World-Wide Standard Seismic Network (WWSSN), the generalized inverse technique was applied to constrain the source parameters and depth of the foreshock, main event, and large aftershock of the September 1963 Lake Kariba sequence (Pavlin and Langston, 1982a). The fault plane solution of the main event is depicted in Figure 8a. The diagram suggests that there are two possible orientations that would account for the observed body-wave data. The latter ambiguity in the strike, dip, and rake is a result of dislocation source theory. In this instance, one can choose between a normal fault ( $\lambda = 270^\circ$ ) that strikes S  $13^\circ$ W with a moderate northwest dip of  $53^\circ$ , or a normal fault that strikes N  $13^\circ$ E with a shallow southeast dip of  $37^\circ$ . As most of the faults of the Lake Kariba region are normal faults with dips of about  $60^\circ$ , the

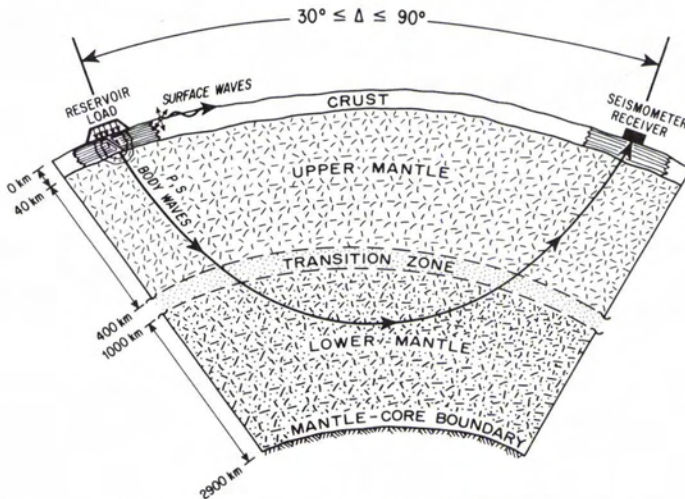


FIG. 7. Schematic of gross Earth structure and the path of seismic body waves to teleseismic receivers. For the distance range of  $30^\circ \leq \Delta \leq 90^\circ$ , P and SH body waves bottom in the lower mantle and experience comparatively little distortion by other Earth structure. As a result, the waveforms of body waves are primarily controlled by the nature of faulting at the source, crustal structure near the source, and, to a lesser extent, crustal structure near the receiver.

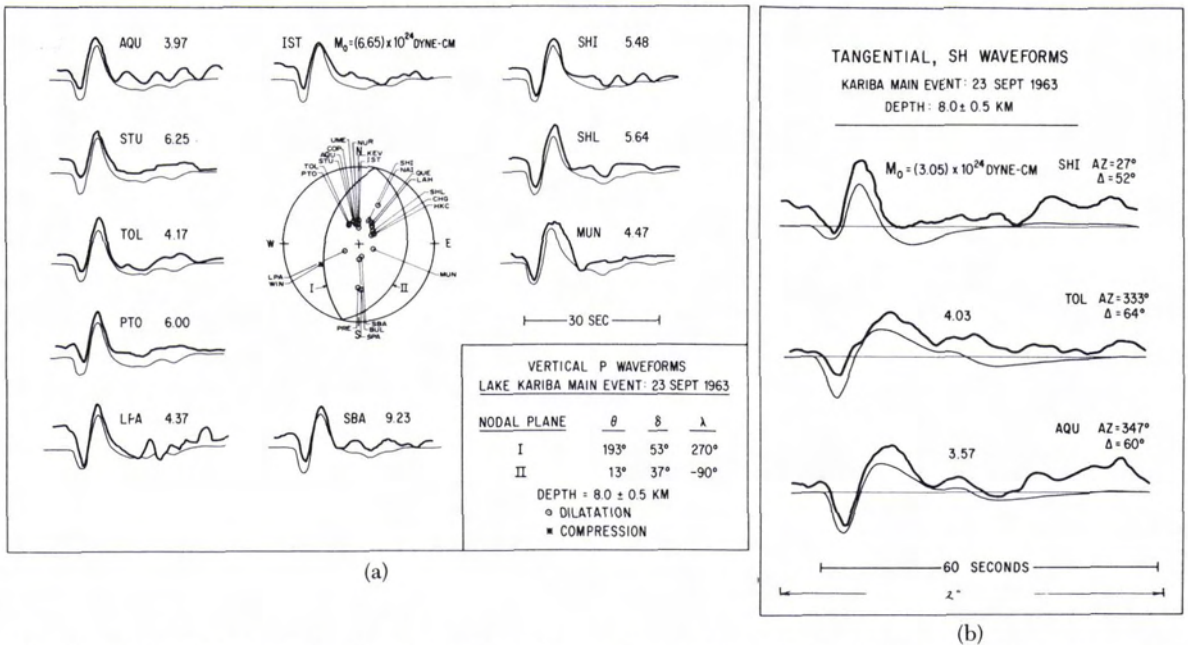


FIG. 8. Results of the inversion of body wave data of the main event at Lake Kariba. (a) Coarse waveforms represent actual P-wave data observed at a given station. Fine-line waveforms are synthetics; their polarity and shape infer a good solution. The representation of the focal sphere in the center of figure represents the mechanism of the earthquake; in this case, a normal fault. The plot is an equal area stereographic projection of the lower hemisphere of the focal sphere. (b) Observed (top) and synthetic (bottom) SH waveforms for the Kariba main event. Although there were only three useful SH wave-forms for this event, these data provided considerable constraint on the fault mechanism because SH radiation is more sensitive to fault orientation than P waves for dip-slip type sources.

former solution was selected. The conventions for strike, dip, and rake can be found in Langston and Helmberger (1975).

The bold-line waveforms of Figure 8a represent the P-wave data recorded at the various WWSSN stations, whereas the fine-line waveforms correspond to synthetic P waves that were generated through the application of generalized ray theory (Langston and Helmberger, 1975). It can be seen that the P-wave data used are confined in azimuth and distance to the central portion of the focal sphere. Obviously, a fault plane solution using only the P first motions would be unconstrained for this event. Inversion of the P waveforms alone would yield a normal fault but with no constraint on strike and little constraint on rake or dip. The mechanism of Figure 8a was strongly constrained by the inclusion of three SH waveforms in the inversion (Figure 8b). SH waves often form very strong constraints on orientation when taken in conjunction with P waves (Langston, 1982). Table 2, lists the solutions achieved for the foreshock, main event, and aftershock of the Lake Kariba sequence. The synthesis of these findings is that the September 1963 earthquakes at Lake Kariba were triggered by normal dip-slip movement along a fault or faults that transected the reservoir. Based upon the joint epicenter determinations reported by Fairhead and Girdler (1969), complemented by the relative event locations derived by the authors,

a model was developed for active fault locations at Lake Kariba.

The September 1963 sequence is believed to have occurred along a common normal fault that transects the Sanyati Basin along a south to southwest azimuth. The foreshock, main event, and aftershock were determined to be shallow earthquakes with depths ranging from 6 to 8 km. The hypothesis of a common fault is based upon the fact that all three events were found to have both comparable source parameters and adjoining epicentral locations.

#### DISCUSSION

Significantly, the orientation of the September 1963 active fault that was associated with Lake Kariba's reservoir-induced earthquakes seems to

TABLE 2. FAULT PARAMETER SOLUTIONS: FORESHOCK, MAIN EVENT, AFTERSHOCK—LAKE KARIBA

Earthquake Time (GMT)	Strike, $\theta$	Dip, $\delta$	Rake, $\lambda$
0640, 23 Sept 63	$188 \pm 5^\circ$	$72 \pm 3^\circ$	$259 \pm 3^\circ$
0901, 23 Sept 63	$193 \pm 8^\circ$	$53 \pm 2^\circ$	$270 \pm 4^\circ$
0703, 25 Sept 63	$188 \pm 3^\circ$	$59 \pm 1^\circ$	$268 \pm 3^\circ$

be aligned subparallel to the orientations of the lineaments located north of the reservoir's Sanyati Basin (Figure 5). If Figures 3 and 5 are compared, a unique "known" fault is observed that approaches the north shore of the Sanyati Basin along a north-south heading. This fault was extended to the north shore of Lake Kariba through photointerpretation of Landsat imagery. Some of the lineaments mapped in Figure 5 may represent the surficial expression of this fault as it transects the Sanyati Basin. Unfortunately, there is no unequivocal proof that this fault actually transects the Sanyati Basin. However, the integrated evidence from field surveys, photo-interpretation, and the location of earthquake epicenters suggests that this fault may indeed control the September 1963 earthquake activity.

Figure 5 also depicts the conjectured extension of a "known" fault, trending N 50°E, across the Sanyati Basin. This suspected fault extension is annotated by the dotted line across the basin. The extension was based upon the presence of a photointerpreted lineament transecting the land located south of the reservoir's central 'neck' region. The presence of the conjectured fault is consistent with the *en echelon* normal faults, trending N 50°E, that bound the Mid-Zambezi Valley. If this fault exists, the Sanyati Basin may be composed of three or more blocks of basement rock capped by sediments of the Karoo formation; each block delineated by a normal fault. The photointerpreted fault extension would probably have a dip consistent with the normal faults of the region. The fault seems to intersect with the active fault, trending S 9°W, controlling the reservoir-induced events of 1963; consequently, the N 50°E fault may also play a role in the triggering of the earthquakes. Only additional field work would confirm the validity of the latter scenario.

At this time, there is good evidence to suggest that the September 1963 reservoir-induced earthquakes of Lake Kariba were triggered along a common normal fault that transects the Sanyati Basin. The foreshock, main event, and aftershock were determined to have occurred at source depths of less than 10 km (Pavlin and Langston, 1982b). By computing an average for the fault plane orientations reported in Table 2, the common fault has an orientation of S 9°W,  $\delta = 62^\circ$ , and  $\lambda = 266^\circ$ . The strike of this fault is consistent with evidence obtained from the photointerpretation of the Landsat imagery of the region (Figures 3 and 5).

It is worth noting that the trend of the inferred active fault is represented in the rose plots of Figure 6, but only in a minor way. If, as a subjunctive possibility, this study of Landsat imagery was performed before lake impoundment, faulting on N 20°W or N 50°E trends would probably have been predicted because these trends are far more obvious. From the geologic evidence alone, the N 50°E trend would have been preferred.

It is not likely, at first glance, that the perturbing effect of the reservoir, either through increased load or increased pore pressure, would preferentially select northward trending normal faults over other trends. Because the compression axis for normal-faulting is near vertical, the stabilizing effect of pure water load on faults directly beneath the reservoir should act equally well for normal faults of any strike (e.g., see Simpson, 1976). Using the conceptual model of a reservoir of infinite extent, stabilization comes about because an increase of vertical stress serves to increase the normal stress on the fault plane. This increases the frictional stress on the fault which must be overcome by the tectonic stress. Indeed, fault stabilization should be maximum for normal fault orientations furthest from those implied by regional tectonic trends.

If a pore pressure change induces faulting (Simpson, 1976; Bell and Nur, 1978), then it would seem that water conduits are more permeable for the northward trending faults than any others. This in turn implies that the north trending faults may be the most active in the region today. Taken together, these two arguments support the straightforward interpretation of the fault parameters that current extensional tectonic stresses are acting in a more east-west direction at present compared to those which caused most of the mapped faults and lineaments.

What, then, do these results imply for the causes of RIS? The primary contribution of the combined use of Landsat imagery and body wave modeling lies in determining basic seismic parameters, such as source location and mechanism, which were previously indeterminate. The shallow source depths obtained in the body wave modeling give credence to the hypothesis that the reservoir triggered the earthquakes. Plausible stress changes caused by impoundment can only be on the order of 0.1 to 10 bars and rapidly fall off with distance. Thus, the probability that an earthquake is "induced" also falls off quickly with distance. These basic fault parameters can serve as constraints on theoretical models of induced seismicity at Lake Kariba. The synthesis of both studies serves as a working model for structure and tectonics in the epicentral area. Our results should serve as a guide for future field studies of seismicity and geology for the region.

#### CONCLUSION

The September 1963 reservoir-induced earthquakes at Lake Kariba were triggered by a shallow normal fault that passes beneath the Sanyati Basin on a S 9°W azimuth. The source depths of the 1963 sequence are less than 10 km. Landsat imagery provided an independent constraint upon the fault parameter solutions that were achieved through the inversion of long- and short-period body-wave data. Pending further analysis, the Sanyati Basin may be comprised of three or more blocks of Pre-

cambrian basement separated by normal faults. Their dynamic adjustment to the reservoir load, complemented by pore pressure effects and *in situ* stresses, may constitute potential triggering mechanisms of the 1963 seismicity.

The lineament patterns mapped from Landsat imagery, if confirmed by more detailed field surveys of the region, may provide additional information on the tectonic history of the region. Furthermore, as reported by Sabins (1978) and Podwysocki (1974), the lineaments and their intersections with known faults of the Lake Kariba region may provide potential sites for future mineral exploration.

#### ACKNOWLEDGMENTS

The authors gratefully acknowledge the comments of Michal Ruder, Charles Bufe, and an anonymous reviewer which served to improve the manuscript. This research was supported by the Division of Earth Sciences of the National Science Foundation under Grant No. EAR-7919915.

#### REFERENCES

- Archer, C., and J. F. Allen, 1979. *A Catalogue of Earthquakes in Lake Kariba Area, 1959-1979*, issued by the Director, Meteorological Services, Salisbury.
- Bell, M., and A. Nur, 1978. Strength Changes due to Reservoir-Induced Pore Pressure and Stresses and Application to Lake Oroville, *Jour. Geophys. Res.*, Vol. 83, 4469-4483.
- Brace, W., 1972. Pore Pressure in Geophysics, *American Geophysical Union Monograph*, 16, 265-273.
- Broderick, T., 1976. *Explanation of the Geological Map of the Country East of Kariba*, Rhodesia Geological Survey Short Report No. 43, Salisbury, 98 p.
- Carder, D., 1945. Seismic Investigations in the Boulder Dam Area, 1940-1944, and the influence of reservoir loading on earthquake activity, *Bull. Seismol. Soc. Am.*, Vol. 35, pp. 175-192.
- Chapman, D., and H. Pollack, 1977. Heat Flow and heat production in Zambia: Evidence for lithospheric thinning in Central Africa, *Tectonophysics*, Vol. 41, pp. 70-100.
- Dahlman, O., and H. Israelson, 1977. *Monitoring underground nuclear explosions*, Elsevier Publishing Company, New York, 440 p.
- Drysdall, A., and R. Weller, 1966. Karoo Sedimentation in Northern Rhodesia, *Trans. Geol. Soc.*, South Africa, Vol. 69, pp. 39-69.
- Engdahl, E. R., and H. Kanamori, 1980. Determination of Earthquake Parameters, *EOS*, Vol. 61, 62-64.
- Fairhead, J., and R. Girdler, 1969. How far does the Rift System extend through Africa, *Nature*, Vol. 221, pp. 1081-1020.
- Gair, H., 1959. The Karoo System and coal resources of the Gwembe District, North-East Section, *Geological Survey of North Rhodesia*, Bulletin No. 1, pp. 1-38.
- Gough, D. I., 1978. Induced Seismicity, Chapter 4, in *The Assessment and Mitigation of Earthquake Risk*, Unesco, New York, 341 p.
- Gough, D., and W. Gough, 1970a. Stress and deflection in the lithosphere near Lake Kariba—I, *Geophysical Journal of the Royal Astronomical Society*, Vol. 21, pp. 65-78.
- , 1970b. Load-induced earthquakes at Lake Kariba—II, *Geophysical Journal of the Royal Astronomical Society*, Vol. 21, pp. 79-101.
- Gupta, H., and B. Rastogi, 1976. Dams and earthquakes, in *Developments in Geotechnical Engineering*, Vol. 11, Elsevier Scientific Publishing Company, New York, 229 p.
- Gupta, H., B. Rastogi, and H. Narain, 1972. Common Features of the Reservoir-Associated Seismic Activities, *Bulletin of the Seismological Society of America*, Vol. 62, No. 2, pp. 481-492.
- Healy, J., C. Raleigh, and J. Bredehoeft, 1972. Faulting and Crustal Stress at Rangely, Colorado, *American Geophysical Union Monograph*, Vol. 16, pp. 275-284.
- Helmberger, D. V., 1974. Generalized ray theory for shear dislocations, *Bull. Seismol. Soc. Am.*, 64, 45-64.
- Helmberger, D. V., and L. J. Burdick, 1979. Synthetic Seismograms, *Am. Rev. Earth Planet. Sci.*, 7, 417-442.
- Hitchon, B., 1958. *The Geology of the Kariba Area*, Report No. 3, Geological Survey Department of Northern Rhodesia, Lusaka, 41 p.
- Holben, B., and C. Justice, 1980. Topographic Effect on Spectral Response from Nadir-Pointing Sensors, *Photogrammetric Engineering and Remote Sensing*, Vol. 46, pp. 1191-1200.
- Hurley, P., 1968. The Confirmation of Continental Drift, *Scientific American*, Vol. 218, No. 4, pp. 52-64.
- Kisslinger, C., 1976. A Review of the Theory of Mechanisms of Induced Seismicity, *Engineering Geology*, Vol. 10, pp. 85-96.
- Langston, C., 1981. Source Inversion of Seismic Waveforms: The Koyna, India, Earthquakes of 13 September 1967, *Bull. Seismol. Soc. Am.*, Vol. 71, No. 1, pp. 1-24.
- , 1982. Single-station fault plane solutions, *Bull. Seismol. Soc. Am.*, Vol. 71, No. 1, pp. 117-130.
- Langston, C., and D. Helmberger, 1975. A Procedure for Modelling Shallow Dislocation Sources, *Geophysical Journal of the Royal Astronomical Society*, Vol. 42, pp. 117-130.
- McConnell, R., 1970. The Evolution of the Rift System of Eastern Africa in the Light of Wegmann's Concept of Tectonic Levels, in *Graben Problems: International Upper Mantle Project Scientific Report #27*, J. H. Illies and St. Mueller (editors), E. Schweizerbart Publishing Company, Stuttgart, pp. 285-290.
- Pavlin, G., and C. Lanston, 1982a. Source Parameter Inversion of a Reservoir-Induced Seismic Sequence: Lake Kariba, Africa (September, 1963), *Geophysical Journal of the Royal Astronomical Society*, submitted for publication.

- , 1982b. Source Depth Determination Using Multimodal Rayleigh Spectral Ratios and Linear Discriminant Analysis: A Study of the Reservoir-Induced Seismic Sequence at Lake Kariba, Africa, (September 1963—August 1974), *Bulletin of the Seismological Society of America*, submitted for publication.
- Podwysocki, M., 1974. *The Relationships of Fracture Traces to Geologic Parameters in Flat-Lying Sedimentary Rocks: A Statistical Analysis*, Ph.D. Thesis, The Pennsylvania State University, 150 p.
- Sabins, F., 1978. *Remote Sensing—Principles and Interpretation*, W. H. Freeman and Company, San Francisco, 426 p.
- Simpson, D., 1976. Seismicity Changes Associated with Reservoir Loading, *Engineering Geology*, Vol. 10, pp. 123-150.
- Smith, A., 1963. *The Geology of the Country around Mazabuka and Kafue*; Ministry of Labour and Mines, North Rhodesian Geological Survey Report No. 2, Lusaka, 32 p.
- Snow, D., 1974. *The geologic, hydrologic, and geomorphic setting of the earthquakes at Lake Kariba*. Final Report: U.S. Geological Survey Earthquake Generation Program, Advanced Research Projects Agency (ARPA), Contract No. 14-08-001-13079, 45 p.
- Stagman, J., 1978. *An Outline of the Geology of Rhodesia*, Rhodesian Geological Survey Bulletin, No. 80, Salisbury, 126 p.
- Wahlstrom, E., 1974. Mechanics of Dam Foundations, in *Developments in Geotechnical Engineering*, Elsevier Publishing Company, Vol. 6, New York, pp. 165-184.
- Wiggins, R., 1972. The General Linear Inverse Problem: Implications of Surface Waves and Free Oscillations for Earth Structure, *Reviews in Geophysics and Space Physics*, Vol. 10, pp. 251-285.

(Received 13 August 1981; revised and accepted 1 January 1983)

## 1983 Engineering Summer Conferences

The University of Michigan  
Ann Arbor, Michigan

### 13-17 June 1983—Infrared Technology: Fundamentals and System Applications

Presentations cover radiation theory, radiative properties of matter, atmospheric propagation, optics, and detectors. System design and the interpretation of target and background signals are emphasized.

### 20-24 June 1983—Advanced Infrared Technology

Presentations cover atmospheric propagation, detectors and focal plane array technology, discrimination characteristics of targets and background, and system designs.

### 27 June-1 July 1983—Synthetic Aperture Radar Technology and Applications

Topics covered include range-doppler imaging of rotating objects, spotlight radar concepts, bistatic radar, and the technology used in optical and digital processing of SAR data for terrain mapping.

For further information please contact

Continuing Engineering Education  
300 Chrysler Center, North Campus  
Ann Arbor, MI 49108  
Tele. (313) 764-8490